Article

Solid-State NMR on a Type III Antifreeze Protein in the Presence of Ice

Ansgar B. Siemer, and Ann E. McDermott

J. Am. Chem. Soc., **2008**, 130 (51), 17394-17399 • DOI: 10.1021/ja8047893 • Publication Date (Web): 02 December 2008

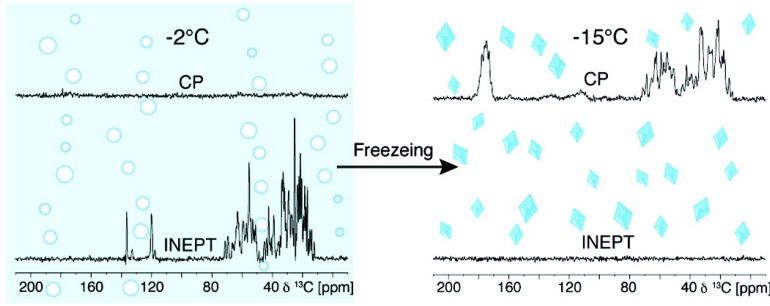

J|A|C|S
ARTICLES

Published on Web 12/02/2008

Solid-State NMR on a Type III Antifreeze Protein in the Presence of Ice

Ansgar B. Siemer* and Ann E. McDermott

Department of Chemistry, MC3113, Columbia University, New York, New York 10027

Received June 23, 2008; E-mail: as3211@columbia.edu

Abstract: Antifreeze proteins (AFPs) are found in fish, insects, plants, and a variety of other organisms where they serve to prevent the growth of ice at subzero temperatures. Type III AFPs cloned from polar fishes have been studied extensively with X-ray crystallography, liquid-state NMR, and site directed mutagenesis and are, therefore, among the best characterized AFPs. A flat surface on the protein has previously been proposed to be the ice-binding site of type III AFP. The detailed nature of the ice binding remains controversial since it is not clear whether only polar or also hydrophobic residues are involved in ice binding and there is no structural information available of a type III AFP bound to ice. Here we present a high-resolution solid-state NMR study of a type III AFP (HPLC-12 isoform) in the presence of ice. The chemical-shift differences we detected between the frozen and the nonfrozen state agree well with the proposed ice-binding site. Furthermore, we found that the ^{1}H T_1 of HPLC-12 in frozen solution is very long compared to typical ^{1}H of proteins in the solid state as for example of ubiquitin in frozen solution.

1. Introduction

Antifreeze proteins (AFPs) are expressed in fish, insects, plants, bacteria and other organisms, where they contribute to both freeze resistance and freeze tolerance. AFPs form a structurally diverse class of proteins including purely α-helical, mixed α-helical/β-sheet, purely β, and antifreeze glycoproteins (AFGPs).[1] AFPs bind to ice and inhibit its growth, thereby lowering the freezing point below the melting point in a nonequilibrium fashion known as thermal hysteresis.[2]

One of the best studied AFPs is type III AFP from arctic fish. Type III AFPs are small, globular, mixed α-β proteins of 62−66 amino acids. High-resolution X-ray and liquid-state NMR structures of a type III AFP called HPLC-12,[3−7] together with site-directed mutagenesis experiments[4,8−11] and molecular dynamics (MD) simulations,[3,5] suggested an ice-binding site for the type III AFP isoform HPLC-12. This putative ice-binding site is formed by a flat surface of the protein and comprises residues Gln9, Leu10, Pro12, Ile13, Asn14, Thr15, Ala16, Thr18, Val20, Met21, Val41, Ser42, Gln44, and Lys61. The residues of this surface point into the solvent and have no obvious role for the stability of the structure. Ice-etching experiments showed that type III AFP binds to several different ice planes.[3] The irreversibility of the type III AFP−ice interaction was recently demonstrated with fluorescence microscopy.[12]

Many high-resolution atomic structures of AFPs were determined by solution NMR and by X-ray crystallography. The X-ray structures of type III AFP included water molecules, but even those obtained at low temperatures did not contain ordered ice.[3,4] Thus no structural information is available for AFPs bound to ice. Except for the mutagenesis experiments, showing the importance of some residues for the antifreeze activity, there are no experimental data that directly confirm the proposed ice binding site of type III AFP.

Solid-state NMR is an ideal tool to measure the structural changes of AFPs upon ice binding, because it can provide atomic-resolution structural information without the need for crystals or soluble protein. Solid-state NMR studies on proteins in frozen solution were done to investigate protein folding,[13] peptide protein complexes,[14] and conformational disorder. Most of these studies were done on flash-frozen H_2O/glycerol solutions to prevent ice formation. Greather et al. showed that type I AFP can form amyloid fibrils during repetitive freezing and thawing. They investigated the effect of type I AFP mutants on their structural and dynamical behavior close to and below

(1) Jia, Z.; Davies, P. L. *Trends Biochem. Sci.* **2002**, *27*, 101–106.
(2) Kristiansen, E.; Zachariassen, K. E. *Cryobiology* **2005**, *51*, 262–280.
(3) Antson, A. A.; Smith, D. J.; Roper, D. I.; Lewis, S.; Caves, L. S.; Verma, C. S.; Buckley, S. L.; Lillford, P. J.; Hubbard, R. E. *J. Mol. Biol.* **2001**, *305*, 875–889.
(4) Jia, Z.; DeLuca, C. I.; Chao, H.; Davies, P. L. *Nature* **1996**, *384*, 285–288.
(5) Yang, D. S.; Hon, W. C.; Bubanko, S.; Xue, Y.; Seetharaman, J.; Hew, C. L.; Sicheri, F. *Biophys. J.* **1998**, *74*, 2142–2151.
(6) Sönnichsen, F. D.; Sykes, B. D.; Chao, H.; Davies, P. L. *Science* **1993**, *259*, 1154–1157.
(7) Sönnichsen, F. D.; DeLuca, C. I.; Davies, P. L.; Sykes, B. D. *Structure* **1996**, *4*, 1325–1337.
(8) Chao, H.; Sönnichsen, F. D.; DeLuca, C. I.; Sykes, B. D.; Davies, P. L. *Protein Sci.* **1994**, *3*, 1760–1769.
(9) Chen, G.; Jia, Z. *Biophys. J.* **1999**, *77*, 1602–1608.
(10) Graether, S. P.; DeLuca, C. I.; Baardsnes, J.; Hill, G. A.; Davies, P. L.; Jia, Z. *J. Biol. Chem.* **1999**, *274*, 11842–11847.
(11) Baardsnes, J.; Davies, P. L. *Biochim. Biophys. Acta* **2002**, *1601*, 49–54.
(12) Pertaya, N.; Marshall, C. B.; Diprinzio, C. L.; Wilen, L.; Thomson, E. S.; Wettlaufer, J. S.; Davies, P. L.; Braslavsky, I. *Biophys. J.* **2007**, *92*, 3663–3673.
(13) Havlin, R. H.; Tycko, R. *Proc. Natl. Acad. Sci. U.S.A.* **2005**, *102*, 3284–3289.
(14) Sharpe, S.; Kessler, N.; Anglister, J. A.; Yau, W.-M.; Tycko, R. *J. Am. Chem. Soc.* **2004**, *126*, 4979–4990.
(15) Heise, H.; Luca, S.; de Groot, B. L.; Grubm Baldus, M. *Biophys. J.* **2005**, *89*, 2113–2120.

10.1021/ja8047893 CCC: $40.75

the freezing point, the latter also with solid-state NMR.[16,17] Ba and co-workers investigated the dynamics and reversibility of type I AFP's ice binding using liquid- and solid-state NMR,[18,19] and Tsvetkova et al. investigated the dynamics of an AFGP using solid-state NMR.[20] All these studies were done on site-specifically isotope labeled or natural abundance protein samples using one-dimensional (1D) solid-state NMR techniques. Here we present a study of a fully $^{13}C-^{15}N$ labeled type III AFP in frozen solution using a high-resolution solid-state NMR approach.

2. Materials and Methods

Expression and Purification. The pET-20 vector with His-tagged type III AFP isoform HPLC-12 was kindly provided by Prof. Peter Davies (Queen's University Kingston, Canada). Fully ^{13}C and ^{15}N enriched HPLC-12 was expressed in *E. coli* BL21(DE3) pLysS cells (Invitrogen). After transformation, cells were grown in 4 L of LB medium containing 100 μg/mL ampicillin and 34 μg/mL chloramphenicol at 37 °C shaking at 250 rpm. When an OD_{600} between 0.6−0.8 was reached, the cells were pelleted by centrifugation, washed with 1 L of M9 buffer, and redissolved in 1 L of M9 minimal medium containing 100 μg/mL ampicillin and 34 μg/mL chloramphenicol, 0.5 g of $^{15}NH_2Cl$, and 4 g of ^{13}C labeled glucose. After 1 h of equilibration at 37 °C, the HPLC-12 expression was induced with 1 mM IPTG and the cells were harvested after 12 h of growth at 37 °C.

The following steps were all done on ice or at 4 °C: After redissolving the cells in 120 mL of buffer (10 mM tris, 0.1 mM EDTA, pH 8.0) containing 1 mg/mL lysozyme (Sigma) and 800 μL protease Inhibitor cocktail (Sigma, P8849), the cells were lysed in a French press. Centrifugation for 20 min at 15 000 rpm (JA-17, Beckman Coulter) separated the soluble from the nonsoluble cell fraction. Since HPLC-12 is found in the soluble and nonsoluble fractions of the cell lysate,[21] it was purified from both of these fractions:

The soluble fraction was passed through a 20 μm filter (Millipore) and then loaded to a Ni-NTA agarose (Quiagen) column equilibrated with 50 mM tris, 0.5 M NaCl, 20 mM imidazole (buffer B). After washing the column with buffer B, the protein was eluted with buffer B and an imidazole step gradient (100−250 mM). The protein came off at ∼200 mM imidazole.

The nonsoluble cell lysate was dissolved in 18 mL of 100 mM NaH_2PO_4, 10 mM tris, 6 M guanidine-HCl, pH 8 (lysis buffer), sonicated for 8 min, and centrifuged (15000 rpm) for 30 min, and the supernatant was loaded onto a Ni-NTA agarose column equilibrated with lysis buffer. After washing the column with 100 mL of lysis buffer pH 6.6, the protein was eluted using a pH gradient (pH 5.25−3.75). The protein eluted at ∼pH 4.75.

Protein fractions from both the soluble and nonsoluble cell lysate were dialyzed against H_2O, and their concentration and purity were analyzed using UV spectroscopy (UV-1601, Shimadzu), SDS-PAGE, and mass spectrometry. Finally the pure fractions were lyophilized and stored at −20 °C.

Fully $^{13}C-^{15}N$ enriched ubiquitin was expressed and purified as described elsewhere.[22]

Liquid-State NMR. Liquid-state NMR chemical shifts were referenced using DSS. $^1H-^{15}N$ and $^1H-^{13}C$ HSQCs[23] as well as 3D HNCO,[24] HNCACB,[25] CBCAcoNH,[25] hCccoNH, HcccoNH,[26] and hCCH-TOCSY[27] spectra were recorded on a 600 MHz Bruker liquid-state NMR spectrometer, equipped with a triple-resonance cryo-probe. The HPLC-12 sample had a concentration of 1 mg/mL and a pH of 7 and was measured at a temperature of 24 °C.

Solid-State NMR. All solid-state NMR sample temperatures were calibrated using $Pb(NO_3)_2$.[28] Solid-state NMR ^{13}C chemical shifts were referenced externally relative to DSS using adamantane.[29] The ^{13}C 1D CP-MAS and 2D DARR spectra[30] of HPLC-12 and ubiquitin were recorded on a Bruker 750 MHz spectrometer using a 4 mm triple-resonance HCN probe operating at 12 kHz MAS. Lyophilized HPLC-12 and ubiquitin were dissolved in deionized H_2O leading to a concentration of 34 and 25 mg/mL, respectively. 50 μL of these samples were then packed to 4 mm rotors. The rf-field strengths for the adiabatic ^{13}C CP spectra were 62 and 50 kHz for ^1H and ^{13}C, respectively, and 100 kHz Spinal64[31] ^1H decoupling was used. The 2D DARR spectra of HPLC-12 and ubiquitin were recorded with a mixing time of 20 ms and a spectral width of 50 kHz in both dimensions. 80 respective 48 FIDs were added up for each of the 1024 t_1 increments leading to an overall measurement time of 68 and 41 h for HPLC-12 and ubiquitin, respectively. For the DARR spectrum of ubiquitin the initial magnetization was coming from a $^1H-^{13}C$ CP; however, for HPLC-12 direct excitation was used to circumvent the long ^1H T_1.

The ^{13}C and ^1H T_1 measurements were done on a 400 MHz Varian Infinityplus spectrometer. The protein concentration was 17 mg/mL for HPLC-12 and 25 mg/mL for ubiquitin in this case. The samples were spun at 9 kHz MAS at a temperature of −35 °C. The CP rf-field strengths were 59 and 50 kHz for ^1H and ^{13}C, respectively, and 100 kHz TPPM ^1H[32] decoupling was used.

Data were processed using Topspin 1.3 (Bruker) or NMRPipe,[33] and multidimensional spectra were analyzed using CARA 1.8.[34] Figure 6 was generated using the VMD software package.[35]

3. Results

The AFP III investigated in this study is the modified HPLC-12 (SWISS-PROT database code ANP12_MACAM) variant from *Macrozoarces americanus* (Ocean pout) where the residues YPPA at the C-terminus were replaced by YAALE+6His to facilitate purification. Similar constructs were used for earlier structural studies on HPLC-12.[3−7] To check the quality of our protein, and as a reference for our solid-state NMR spectra, we first assigned ^1H, ^{13}C, and ^{15}N chemical shifts of uniformly

(16) Graether, S. P.; Slupsky, C. M.; Sykes, B. D. *Biophys. J.* **2003**, *84*, 552–557.
(17) Graether, S. P.; Slupsky, C. M.; Sykes, B. D. *Proteins* **2006**, *63*, 603–610.
(18) Ba, Y.; Wongskhaluang, J.; Li, J. *J. Am. Chem. Soc.* **2003**, *125*, 330–331.
(19) Mao, Y.; Ba, Y. *Biophys. J.* **2006**, *91*, 1059–1068.
(20) Tsvetkova, N. M.; Phillips, B. L.; Krishnan, V. V.; Feeney, R. E.; Fink, W. H.; Crowe, J. H.; Risbud, S. H.; Tablin, F.; Yeh, Y. *Biophys. J.* **2002**, *82*, 464–473.
(21) Chao, H.; Davies, P. L.; Sykes, B. D.; Sönnichsen, F. D. *Protein Sci.* **1993**, *2*, 1411–1428.
(22) Wand, A. J.; Urbauer, J. L.; McEvoy, R. P.; Bieber, R. J. *Biochemistry* **1996**, *35*, 6116–6125.
(23) Schleucher, J.; Schwendinger, M.; Sattler, M.; Schmidt, P.; Schedletzky, O.; Glaser, S. J.; Sørensen, O. W.; Griesinger, C. *J. Biomol. NMR* **1994**, *4*, 301–306.
(24) Kay, L.; Xu, G.; Yamazaki, T. *J. Magn. Reson.* **1994**, *A109*, 129–133.
(25) Muhandiram, D.; Kay, L. *J. Magn. Reson.* **1994**, *103*, 203–216.
(26) Grzesiek, S.; Anglister, J.; Bax, A. *J. Magn. Reson.* **1993**, *101*, 114–119.
(27) Kay, L.; Xu, G.; Singer, A.; Muhandiram, D.; Forman-Kay, J. D. *J. Magn. Reson.* **1993**, *B101*, 333–337.
(28) Bielecki, A.; Burum, D. P. *Journal of Magnetic Resonance A* **1995**, *116*, 215–220.
(29) Morcombe, C. R.; Zilm, K. W. *J. Magn. Reson.* **2003**, *162*, 479–486.
(30) Takegoshi, K.; Nakamura, S.; Terao, T. *Chem. Phys. Lett.* **2001**, *344*, 631–637.
(31) Fung, B. M.; Khitrin, A. K.; Ermolaev, K. *J. Magn. Reson.* **2000**, *142*, 97–101.
(32) Bennett, A. E.; Rienstra, C. M.; Auger, M.; Lakshmi, K. V.; Griffin, R. G. *J. Chem. Phys.* **1995**, *103*, 6951–6958.
(33) Delaglio, F.; Grzesiek, S.; Vuister, G. W.; Zhu, G.; Pfeifer, J.; Bax, A. *J. Biomol. NMR* **1995**, *6*, 277–293.
(34) Keller, R. L. J. *The Computer Aided Resonance Assignment Tutorial*; Cantina, Goldau, 2004.
(35) Humphrey, W.; Dalke, A.; Schulten, K. *J. Mol. Graph.* **1996**, *14*, 33–8.

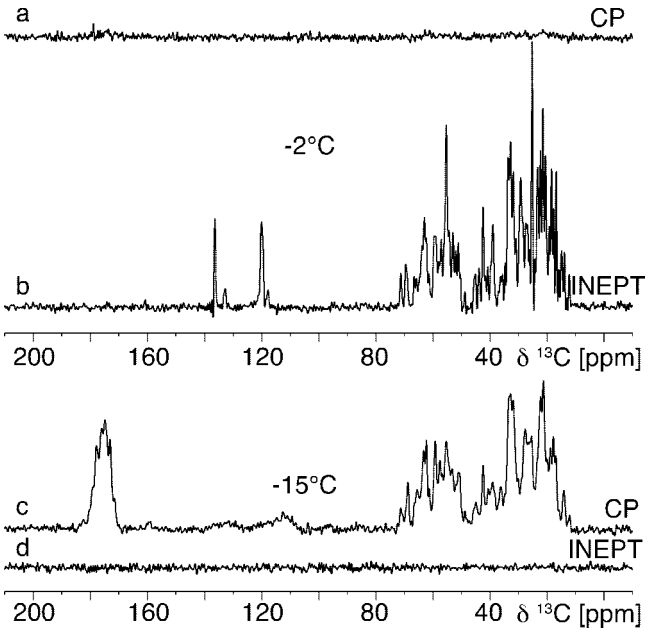

Figure 1. ^{13}C spectra of the uniformly $^{13}C-^{15}N$ labeled type III AFP isoform HPLC-12 in H_2O recorded at 12 kHz MAS on a 750 MHz spectrometer using Spinal64 decoupling. 128 scans were recorded for each of the spectra. (a) Hartmann−Hahn cross polarization (CP) spectrum at −2 °C sample temperature, (b) refocused INEPT spectrum at −2 °C, (c) CP spectrum at −15 °C, (d) refocused INEPT spectrum at −15 °C.

$^{13}C-^{15}N$ labeled HPLC-12 in the liquid state. Sequence specific backbone and side-chain assignments were obtained by analyzing a set of 2D ($^1H-^{15}N$, $^1H-^{13}C$ HSQC[23]) and 3D (HNCACB,[25] CBCAcoNH,[25] HNCO,[24] HcccoNH, hCcccoNH,[26] and hCCH-TOCSY)[27] spectra recorded on a 600 MHz spectrometer at 24 °C. Except for the N-terminal Met, the C-terminal His-tag, and the side-chain carbonyls, amides, and aromatic nuclei, we were able to sequentially assign most of the backbone and side-chain resonances (neglecting the His-tag 86%, 86%, and 72% of all ^1H, ^{13}C, and ^{15}N shifts were assigned, respectively. 95% of the backbone resonances were assigned). We then froze concentrated HPLC-12 solutions (34 mg/mL) during magic-angle spinning (MAS) in a 4 mm MAS rotor. We chose to have no cryoprotectant and slow freezing in this study to have ice-crystal formation and HPLC-12 binding the crystal surface. ^{13}C spectra were recorded at several temperature steps using refocused INEPT,[36] direct excitation, and dipolar Hartmann−Hahn cross polarization (CP)[37] experiments.

As can be seen from Figure 1, the spectra at −2 °C (a and b) differ clearly from those recorded at −15 °C (c and d). The two ^{13}C experiments, refocused INEPT and CP, can be used to identify the state of the sample: The INEPT experiment only works in the case of narrow ^1H lines (i.e., in solution or very dynamic systems). The dipolar CP experiment only works if strong dipolar couplings are present, which is not the case if the molecule is tumbling isotropically in solution. The ^{13}C CP spectrum recorded at −2 °C and the refocused INEPT spectrum at −15 °C showed no signal, indicating that the protein was in solution in the first case and frozen in the second. The transition from frozen to nonfrozen as observed by NMR was relatively sharp and happened between −5 and −2 °C.

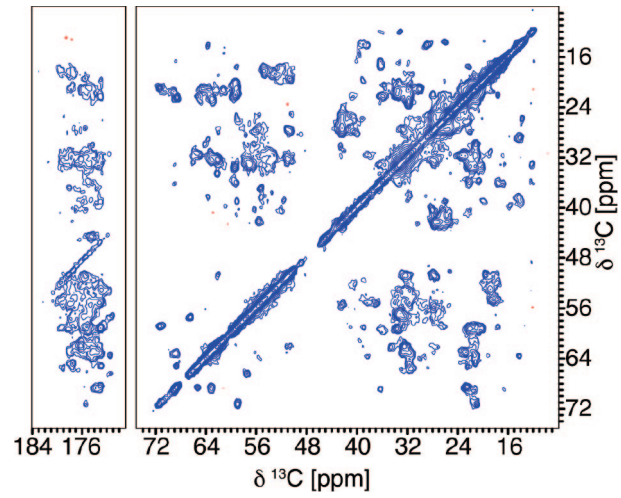

Figure 2. $^{13}C-13C$ DARR spectrum of the frozen (−15 °C) type III AFP isoform HPLC-12 in H_2O at 12 kHz MAS. The spectrum was recorded on a 750 MHz spectrometer with a mixing time of 20 ms.

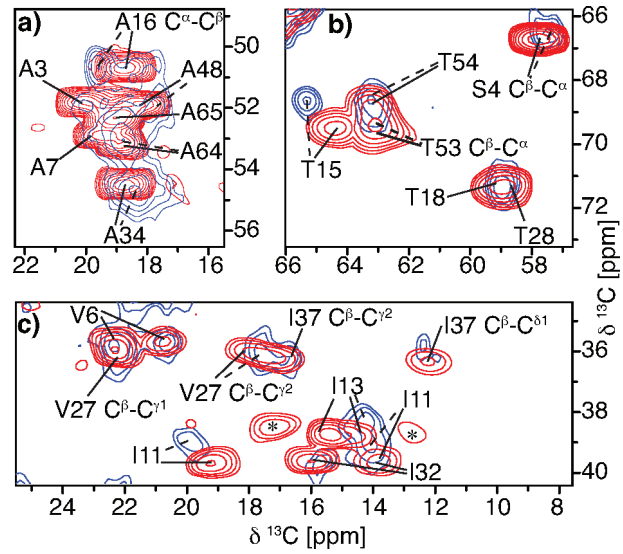

Figure 3. Overlays of 2D $^{13}C-^{13}C$ correlation spectra of the type III AFP isoform HPLC-12 in solution and frozen solution. Enlargements of the 2D DARR spectrum (Figure 2) are shown in blue. The corresponding 2D $^{13}C-^{13}C$ projection of the hCCH-TOCSY recorded on HPLC-12 in solution is shown in red. The resonance assignments of the hCCH-TOCSY spectrum (solid lines) and the solid-state spectrum (dashed lines) are indicated. The asterisks indicate an impurity.

Figure 2 shows a $^{13}C-^{13}C$ 2D DARR spectrum[30] of HPLC-12 recorded at −15 °C. The resolution of this spectrum is comparable to other structurally uniform solid-state NMR protein samples (e.g., crystalline ubiquitine[38] or HET-s(218−289) fibrils)[39] with ^{13}C line widths of clearly less than 1 ppm (i.e., down to 0.4 ppm, 75 Hz). Since many of the cross peaks are resolved, a direct comparison with the ^{13}C chemical shifts of the solution spectra (line widths <30 Hz) is possible. Most chemical-shift assignments agree very well between liquid-state and solid-state spectra. However, some cross peaks are clearly shifted as can be seen in Figure 3. For example Ala16 is shifted in Figure 3a, Thr15 in Figure 3b, and Ile11 in Figure 3c. Val6 in Figure 3c, on the other hand, is an example of the residues that did not shift at all.

(36) Burum, D. P.; Ernst, R. R. *J. Magn. Reson.* **1980**, *39*, 163–168.
(37) Hediger, S.; Meier, B. H.; Kurur, N. D.; Bodenhausen, G.; Ernst, R. R. *Chem. Phys. Lett.* **1994**, *223*, 283–288.
(38) Igumenova, T. I.; McDermott, A. E.; Zilm, K. W.; Martin, R. W.; Paulson, E. K.; Wand, A. J. *J. Am. Chem. Soc.* **2004**, *126*, 6720–6727.
(39) Siemer, A. B.; Ritter, C.; Ernst, M.; Riek, R.; Meier, B. H. *Angew. Chem., Int. Ed.* **2005**, *44*, 2441–2444.

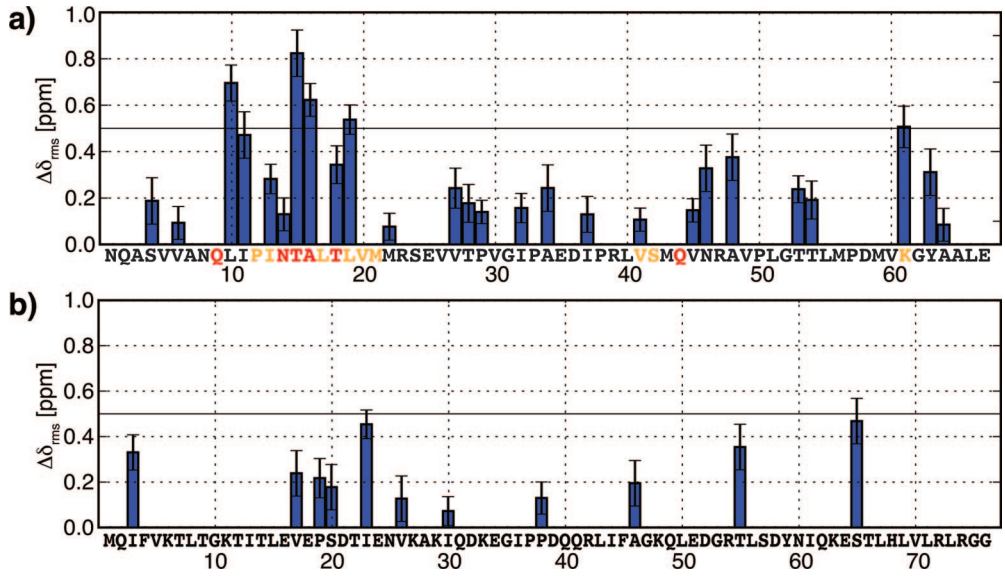

Figure 4. RMS ^{13}C chemical-shift difference $\Delta\delta_{rms} = \Sigma_{i=1}^{N} = [(\delta^i_{sol} - \delta^i_{froz})^2/N]^{1/2}$ for each amino acid is plotted against the protein sequence. (a) HPLC-12. Amino acid residues that were shown to be important for antifreeze activity using site-directed mutagenesis studies and MD simulations are highlighted in red and orange, respectively. (b) Ubiquitin.

To compare the chemical shifts of HPLC-12 between solution and frozen solution in more detail, we projected the liquid-state assignment onto our frozen solution data. Due to the overall good agreement between the data in solution and frozen solution, we saw no need for a *de novo* assignment of the frozen solution spectra. The solution shifts were then manually adjusted so that they fit onto the spectrum in frozen solution. Only obvious adjustments were done, and many of these could be verified using multiple cross peaks belonging to the same spin. For example, the shift of a Thr $C^{\alpha}-C^{\beta}$ cross-peak should also lead to and be consistent with the shifts of the corresponding $C^{\alpha}-C^{\gamma}$, $C^{\beta}-C^{\gamma}$, $C'-C^{\alpha}$, and $C'-C^{\beta}$ cross-peaks.

To illustrate the chemical-shift perturbation per residue, the root-mean-square (RMS) chemical-shift difference $\Delta\delta_{rms}$ for every amino acid was calculated using the following relation:

$$\Delta\delta_{rms} = \sum_{i=1}^{N} \sqrt{(\delta^i_{sol} - \delta^i_{froz})^2/N} \qquad (1)$$

where N is the number of assigned ^{13}C atoms in the amino acid, and δ^i_{sol} and δ^i_{froz} are the ^{13}C chemical shifts in solution and frozen solution, respectively. The carbonyl chemical shifts were omitted in this calculation, because only a few of these were resolved in the 2D DARR spectrum. Figure 4A illustrates this average chemical-shift difference plotted against the amino acid sequence of HPLC-12. The solution assignment of the shifts considered for this plot is virtually complete. Therefore, residues having no entry in this plot showed no visually detectable chemical-shift changes in frozen solution either due to small or no chemical-shift change or because of overlap in the solid-state NMR spectra. Prominent examples of such residues are Q9 and Q44. These residues were shown to be important for ice binding using mutagenesis and MD studies but did not show any detectable chemical-shift changes in our study. This is because amide side chains were not included in our analysis.

We observed the most pronounced chemical-shift changes between residue Leu10 and Leu19, namely for Leu10, Thr15, Ala16, and Leu19 as well as for Lys61. Elsewhere in the sequence the chemical-shift changes were less dramatic.

To check whether the line width and chemical-shift changes observed when freezing HPLC-12 are normal for proteins in frozen solution, we repeated the experiments using human ubiquitin. Ubiquitin is not known to have any noncolligative antifreeze activity and therefore serves as a control in this study. Figure 5 shows the 2D DARR spectrum of a frozen ubiquitin solution recorded under the same conditions as the spectrum shown in Figure 2.

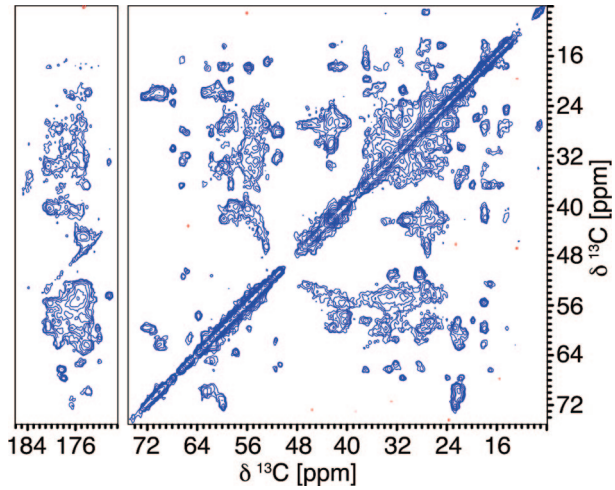

Figure 5. $^{13}C-^{13}C$ DARR spectrum of a frozen (−15 °C) ubiquitin H_2O solution at 12 kHz MAS. The spectrum was recorded on a 750 MHz spectrometer with a mixing time of 20 ms.

The liquid-state NMR shifts of ubiquitin were obtained from the BMRB entry 6466.[22] We analyzed the ^{13}C chemical-shift changes between solution and frozen solution as in the case of HPLC-12 and the results are shown in Figure 4B.

Ubiquitin showed fewer and less pronounced chemical-shift changes than HPLC-12. Furthermore, the amino acids for which chemical-shift changes were detected are distributed uniformly over the sequence of ubiquitin.

Another remarkable difference between HPLC-12 and ubiquitin in frozen solution is the ^1H spin−lattice relaxation time T_1: We measured the general ^1H T_1 by using an inversion recovery sequence before a $^1H-^{13}C$ CP at −35 °C. HPLC-12 has a long ^1H T_1 of ∼7.5 s and ubiquitin a much shorter ^1H T_1

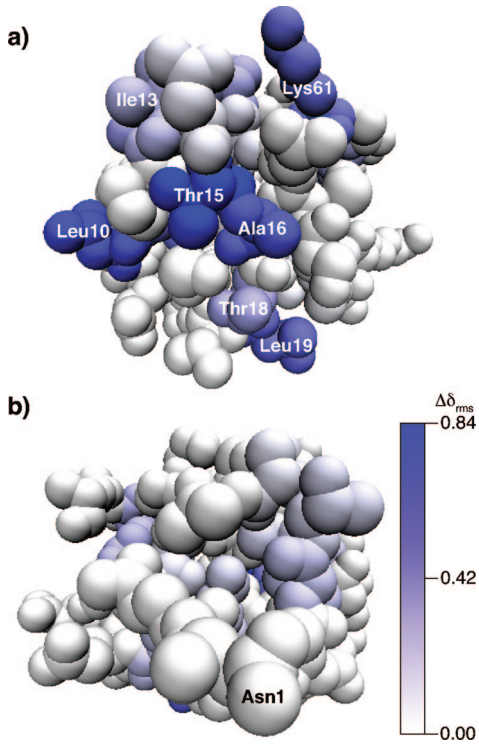

Figure 6. CPK presentation of the solution-state NMR structure of the type III AFP isoform HPLC-12, PDB entry 1KDF.[7] (a) View normal to and displaying the proposed ice-binding surface. Each amino acid is colored uniformly according to its rms ^{13}C chemical-shift change (Figure 4A). White indicates no change, and deep blue indicates maximal chemical-shift change (see color scale on the right side). (b) Same as in (a), but rotated 180° around the vertical axis relative to (a) showing the N-terminal, non-ice-binding site of the protein.

of 0.3 s. We were able to lower T_1 of HPLC-12 to 0.4 s by adding 5 mM of Cu(II)-EDTA to the protein solution.[40,41]

Long ^1H T_1 values of 15 s were also observed by Long and Tycko for a small peptide in frozen solution at −140 °C.[40] They also used Cu(II)-EDTA to shorten the T_1 to ∼1 s. Heise et al. measuring a neurotensin fragment in frozen solution at −50 °C did not report an unusually long ^1H T_1. The remarkable difference in ^1H T_1 between HPLC-12 and ubiquitin we observed could be explained by a difference in protein dynamics, or a difference in structure and dynamics of the surrounding water molecules. We will address this question in our further investigations on HPLC-12.

4. Discussion

HPLC-12 and ubiquitin exhibited line widths in frozen solution of clearly less than 1 ppm. This line width is significantly lower than the line widths measured by other authors on flash-frozen proteins and peptides.[13,15,42] This difference may be attributed in part to the slow freezing of our samples in the magnet under MAS. Another explanation for this difference in line width might be that our spectra were collected on compact, globular proteins, whereas other studies in frozen solution typically employed small peptides[15,42] or protein fibrils.[42]

Most of the ^{13}C chemical shifts of both HPLC-12 and ubiquitin did not change upon freezing, and we conclude that the overall three-dimensional folds of the proteins were not affected by freezing. The few chemical-shift changes observed in ubiquitin were all smaller than 1 ppm and could not be associated with a specific site of the protein. These differences are comparable to or smaller than the chemical differences observed between the solid-state NMR assignment of crystalline ubiquitin and its liquid-state assignment[43] (in fact, the chemical-shift differences of crystalline ubiquitin (BMRB entry 7111) and our shifts in frozen solution are much larger than the differences between solution and frozen solution).

The chemical-shift changes observed for HPLC-12, however, were more sequence specific and pronounced with changes of up to 1.5 ppm. It is important to note that, due to spectral overlap in the frozen state and the omission of ^{15}N and carbonyls in our analysis, not all chemical-shifts changes of HPLC-12 were detected. Therefore, a residue not showing chemical-shift change in Figures 4A and 6 could have changed and been undetected.

As can be seen from Figure 4A the largest chemical-shift changes were detected for amino acids Leu10, Thr15, Ala16, Leu19, and Ile61. All of these residues were proposed to be involved in ice binding in earlier studies.[3,11] Among the residues with a critical role in ice binding, Thr18 showed significant chemical-shift changes. Additional significant chemical-shift changes were detected for residues Ile11, Asn46, Ala48, and Tyr63. These residues were not implicated in ice binding in previous studies.

The ^{13}C chemical-shift changes of up to 1.5 ppm observed in the HPLC-12 binding site are comparable to those observed in previous ligand binding studies using solid-state NMR.[44,45]

The spatial distribution of these chemical-shift perturbations is illustrated in Figure 6. The most pronounced chemical-shift changes are located at the flat surface, which was proposed to be the ice-binding site of HPLC-12.

All chemical-shift changes observed are smaller than the secondary chemical shift (i.e., the difference between the observed and the random-coil chemical shift) indicating that the secondary structure was preserved also in the regions with the largest chemical-shift perturbation. The fact that we observed most of the large chemical-shift changes for side-chain carbons and only Thr15 and Leu19 showed changes in δC^{α} of more than 0.5 ppm underlines that most of the conformational changes happen in the side chains.

Chemical-shift perturbation studies are commonly used to measure protein ligand binding in drug discovery.[46,47] Side-chain chemical shift changes are influenced by ligand binding due to van der Waals interactions and are used to identify the protein side chains involved in ligand binding.

The side-chain chemical-shift changes observed in this study are likewise indicative of the amino acid side chains involved in the ice binding of HPLC-12, which can be looked at as an unusual receptor−ligand interaction.[1]

(40) Long, H. W.; Tycko, R. *J. Am. Chem. Soc.* **1998**, *120*, 7039–7048.
(41) Wickramasinghe, N. P.; Kotecha, M.; Samoson, A.; Past, J.; Ishii, Y. *J. Magn. Reson.* **2007**, *184*, 350–356.
(42) Havlin, R. H.; Blanco, F. J.; Tycko, R. *Biochemistry* **2007**, *46*, 3586–3593.
(43) Igumenova, T. I.; Wand, A. J.; McDermott, A. E. *J. Am. Chem. Soc.* **2004**, *126*, 5323–5331.
(44) Zech, S. G.; Olejniczak, E.; Hajduk, P.; Mack, J.; McDermott, A. E. *J. Am. Chem. Soc.* **2004**, *126*, 13948–13953.
(45) Lange, A.; Giller, K.; Hornig, S.; Martin-Eauclaire, M. F.; Pongs, O.; Becker, S.; Baldus, M. *Nature* **2006**, *440*, 959–962.
(46) Roberts, G. *Drug Discovery Today* **2000**, *5*, 230–240.
(47) Pellecchia, M.; Sem, D. S.; Wüthrich, K. *Nat. Rev. Drug Discovery* **2002**, *1*, 211–219.

5. Conclusion

In this study we presented spectra of the type III AFP isoform HPLC-12 and human ubiquitin in frozen solution. The line widths of both proteins is so narrow in the frozen state that it permits a direct comparison of the ^{13}C chemical shifts between solution and frozen solution. Where there were only small changes detected in the case of ubiquitin, the spectra of HPLC-12 in frozen solution exhibited pronounced chemical-shift changes between residues 10 and 20. These residues thus seam to form the ice-binding interface of HPLC-12 which agrees well with earlier studies of this protein. Furthermore, we found that the ^1H T_1 relaxation time in frozen solution of HPLC-12 is very different from that of ubiquitin. The origin of this difference is not clear to us yet.

Acknowledgment. We would like to thank Prof. Peter Davies for providing us with the HPLC-12 plasmid, Shibani Bhattacharya and Boris Itin for technical assistance in the NMR data collection, as well as Simone Gieschler and Kuo-Ying Huang for useful suggestions and help during the sample preparation. A.B.S. acknowledges a postdoctoral stipend from the Ernst Schering Foundation.

Supporting Information Available: HPLC-12 solution ^1H, ^{13}C, and ^{15}N chemical shifts (ID 15817) as well as ^{13}C chemical shifts in frozen solution (ID 15818) are avaiable from the Biological Magnetic Resonance Data Bank (http://www.bmrb.wisc.edu). Temperature series of direct excitation spectra of HPLC-12 (Figure S1); refocused INEPT and CP 1D ^{13}C spectra of human ubiquitin in solution and frozen solution (Figure S2); inversion−recovery T_1 measurements of HPLC-12 and ubiquitin in frozen solution (Figure S3); change in secondary ^{13}C chemical-shift of HPLC-12 between solution and frozen solution (Figure S4); δ_1 slices through the 2D DARR spectrum of Figure 2 to illustrate the line widths of HPLC-12 in frozen solution (Figure S5). This material is available free of charge via the Internet at http://pubs.acs.org.

JA8047893